Late-onset *NPM1* mutation in a MYC-amplified relapsed/refractory acute myeloid leukemia patient treated with gemtuzumab ozogamicin and glasdegib

In March 2020, a 72-year-old male patient with no relevant medical history presented with 4 weeks of asthenia and adynamia, 10-kg weight loss and petechias on both hands. Examination of the bone marrow (BM) revealed 80% infiltration by immature blastoid cells with the following immune phenotype: low-intermediate CD45 expression, $CD34^{+/-}$, $CD117^{+}$, $HLA\text{-}DR^{+}$, $CD38^{+}$, $CD13^{+/-}$, $CD33^{-/+}$, myeloperoxidase $(MPO)^{-/+}$, $CD15^{-/+}$, $nuTdt^{-/+}$, $CD123^{-/+}$, $CD7^{+}$. In the next-generation sequencing (NGS) acute myelogenous leukemia (AML) panel only one mutation in *TET2* p.Y1245Lfs*22 was reported. Fluorescence *in situ* hybridization (FISH) identified a *MYC* amplification, characterized by double minutes (dmin) involving chromosome band 8q24 in 71% of uncultured BM cells. The disease was classified as AML not otherwise specified (AML-NOS) according to Eurpoean Leukemia Net (ELN) 2017 criteria.[1] Intensive treatment within the "GnG" trial was initiated after obtaining the patient´s written informed consent comprising gemtuzumab-ozogamicin and "7+3" during induction and the hedgehog inhibitor glasdegib during consolidation and maintenance therapy.[2] The course of events is described in detail in Figure 1. Glasdegib maintenance therapy was prematurely discontinued after three cycles due to persistent dysgeusia. For this specific type of AML, no targeted maintenance therapy had been approved in the European Union at that time. However, cytologic relapse occurred 3 months after the suspension of glasdegib with 60% BM blasts (Figure 1). NGS revealed several new molecular mutations including a typical *NPM1* 4bp insertion (Table

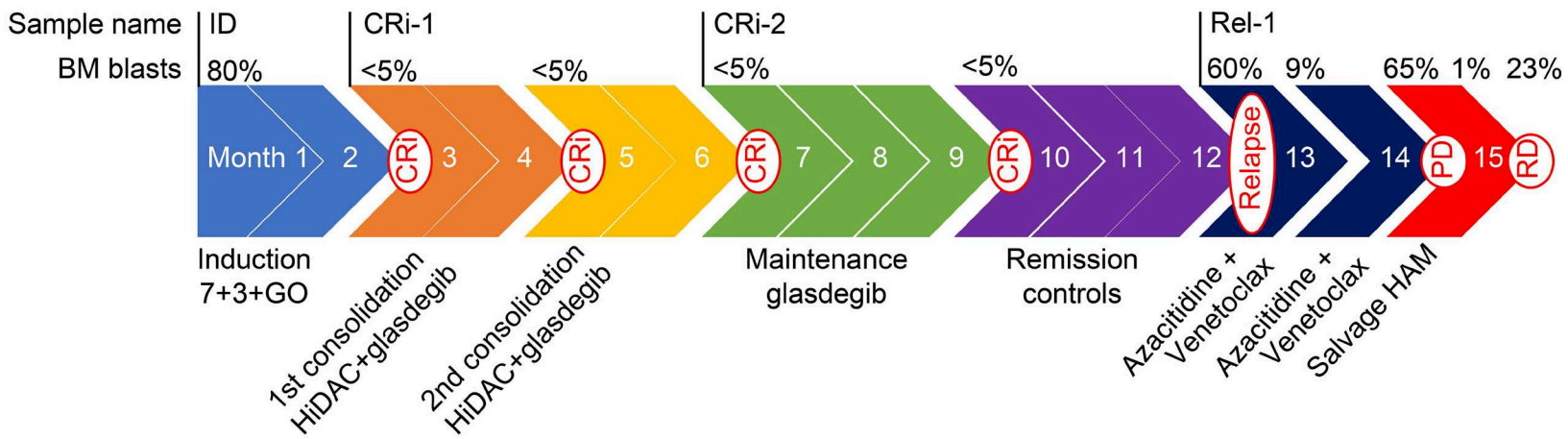

Figure 1. Timeline of therapy, clinical response, and sampling time points. The patient was randomized to receive gemtuzumab ozogamicin (GO) in addition to "7+3" during induction therapy as follows: cytarabine 200 mg/m^2 administered via continuous intravenous (IV) infusion for a total of 7 days and daunorubicin 60 mg/m^2 days 1, 2, and 3; in addition GO 3 mg/m^2 IV over 1 hour (h), on days 1, 4, and 7. During the consolidation phase, the patient received 2 cycles of cytarabine (1.0 g/m^2) administered by IV infusion every 12 h on days 1, 2, and 3. Glasdegib 100 mg was administered from day 1 to 28 of each consolidation cycle. Maintenance therapy with glasdegib 100 mg was started after the end of the second consolidation therapy cycle for a total of 3 additional cycles of 28 days each.[2] The patient achieved complete hematological remission with incomplete hematological recovery (CRi) after induction. Minimal residual disease (MRD) assessed by flow cytometry remained positive. After the first consolidation therapy, CR with MRD negativity was achieved. At this point, an allogeneic transplantation was disclaimed by the patient. Thus, a second cycle of consolidation therapy was administered. Maintenance therapy with glasdegib was initiated 5 months after induction therapy. Glasdegib was prematurely discontinued after 3 cycles of maintenance therapy due to the patient's wish because of adverse effects (dysgeusia and muscle cramps grade II). Cytologic relapse occurred 3 months after the suspension of glasdegib. Bone marrow (BM) examination revealed 60% blasts. Flow cytometry analysis showed a leukemia population with the following characteristics: $CD34^{-}$, $CD117^{-}$, $HLA\text{-}DR^{+}$, $CD38^{+}$, $CD33^{+}$, $CD13^{-/+}$, $CD64^{+}$, $NG2^{+}$, $CD15^{+}$ and a second population displaying the initial immunophenotype. Next-generation sequencing revealed molecular aberrations not detected at initial diagnosis. The *NPM1-mut/ABL* ratio quantified by real-time polymerase chain reaction was 520%. Salvage therapy with azacitidine and venetoclax (aza-ven) was initiated. After 1 cycle, blast percentage dropped to 9%. A second cycle of aza-ven was administered and the patient was prepared for allogeneic transplantation. BM aspiration after the second cycle of aza-ven revealed refractory disease with 60% blasts and an *NPM1-mut/ABL* ratio of 416%. Another salvage therapy with high-dose cytarabine and mitoxantrone (HAM) was initiated. Day +15 BM aspiration revealed only 1% blasts but MRD positivity for *NPM1*. The patient did not achieve hematological recovery, and on day 35, the patient presented with 23% BM blasts. In addition, he developed progressive skin papules suspicious of chloroma covering the entire body, and skin biopsy confirmed AML cell infiltration. Best supportive care therapy was initiated. The patient died 2 months later. CRi: complete remission with incomplete hematological recovery, ID: initial diagnosis; CRi-1: complete remission with incomplete hematological recovery one; CRi-2: complete remission with incomplete hematological recovery two; Rel-1: relapse one; PD: progressive disease; RD: refractory disease.

1). FISH analysis showed the initial *MYC* amplification in 1% of uncultured BM cells, however a new trisomy 8 involving the *MYC* locus (8q24) occurred. We initiated salvage therapy with azacitidine and venetoclax (aza-ven)[3] and prepared the patient for allogeneic stem cell transplantation. However, BM aspiration after the second cycle revealed refractory disease with 60% blasts and persistent *NPM1* mutational load. Another salvage therapy with high-dose cytarabine and mitoxantrone (HAM) was initiated, but the disease was refractory with novel extramedullary skin lesions. Considering the poor prognosis of this chemo-refractory disease, as well as the patient's age and wish a best supportive care therapy was initiated. The patient died 2 months after the appearance of the skin lesions.

In order to gain a deeper understanding of the clonal composition and evolution of this unusual course of the disease, we performed single-cell DNA sequencing (scSeq) at four time points indicated in Figure 1 and Table 1 using the Mission Bio Tapestri single-cell DNA and protein sequencing platform investigating genes covered in Mission Bio's myeloid panel[4] with v2 of the protocol. Additionally, we used antibodies against four surface proteins to simultaneously generate a single-cell protein library. Libraries were sequenced to a DNA/protein read depth of 324/31 M (ID), 267/31 M (CRi-1), 292/37 M (CRi-2) and 225/37 M (Rel-1) on an Illumina NextSeq2000 sequencer (P3, 2x150bp). Sequencing details are available upon request. Using scSeq, we were able to confirm the *MYC* amplification at initial diagnosis in a large fraction of $CD34^+$ blasts. In order to discern *MYC*-amplified from wild-type cells, we used CloneTracer to assign clonal probabilities to each cell.[5] Those cells being assigned to the MYC clone were termed MYC-amplified (*MYC*amp) (Figure 2A). Notably, healthy T cells were reliably identified as non-*MYC*amp as expected (Figure 2A). We identified an *EZH2* missense mutation p.T683A in $CD34^+$ cells with aberrant CD7 expression, which seemed to be present in the *MYC*amp and also non-*MYC*amp $CD34^+CD7^+$ cells, but not in healthy $CD3^+CD34^-$ T cells. This suggested that the *EZH2* mutation occurred in an ancestral committed progenitor cell giving rise to the *MYC*amp leukemic clone (Figure 2B, C). Moreover, an *ASXL1* p.E635Rfs mutation was detected in around 1% of the cells not harboring *MYC*amp (Figure 2B, C).

In the remission sample post induction (CRi-1), which was considered measurable residual disease (MRD)-negative by flow cytometry, the *EZH2* mutation was present in the majority of $CD3^-$ BM cells, but *MYC*amp was detectable in a minority of cells (Figure 2D). However, we identified a *JAK2* V617F mutation typically found in myeloproliferative neoplasms (MPN) and AML,[6] in 9% of the cells, and the *ASXL1* mutation had increased in frequency. Notably, we observed a high allelic dropout rate of *EZH2*, suggesting that many cells called as *EZH2* wild-type were actually mutant, and that the overall fraction of *EZH2* mutant myeloid cells was very high. Considering also that the false-positive rate of the applied technology is very low,[7,8] the abundant co-occurrence of the *ASXL1* and *EZH2* mutations in the first remission time point

Table 1. Clonal composition and evolution of the disease.

	Clinical time point	Karyotype	Blast count bone marrow %	*MYC*amp (FISH) %	*MYC*amp scSeq	*ASXL1* p.Glu635Rfs	*ASXL1* p.Glu635fs COSM36165	*EZH2* p.Thr683Ala %	*EZH2* p.Tyr646Cys	*JAK2* p.Val617Phe COSM12600	NPM1 p.Trp288fs COSM17559	*PHF6* p.Tyr103stop	*TET2* p.Try1245fs COSM87129 %
Clinical diagnostics	Diagnosis (ID)	46,XY,del(16)(p13.1),1~19dmin[13]/46,XY,del(16)(p13.1)[3]/46,XY, 2~15dmin[3]/46,XY[1]	80	71	-	-	-	48*	-	-	-	-	49
	Relapse (Rel-1)	48,XY,+8,+19,2~4dmin[11]/49,sl,+8[2]/46,XY,inv(16)(p11.2q22)[4]/46,XY[3]	60	2	-	3	-	34	-	9	11	-	48
	Progressive disease		65	18 +8	-	-	-	20	27	10	31	-	49
scSeq	Diagnosis (ID)		67 PB	-	72	-	1	80	-	-	-	-	-
	CRi-1		4	-	0	-	42	47	-	8	-	-	-
	CRi-2		<5	-	1	-	6	64	-	23	-	10	-
	Relapse (Rel-1)		60	-	12	-	18	51	-	6	15	19	-

*Not reported initially by clinic, probably because no COSMIC initial diagnosis (ID) and near 50% so considered single-nucelotide polymorphism. *MYC*amp: *MYC*-amplified; FISH: fluorescence *in situ* hybridization; Rel-1: relapse one; PB: peripheral blood; Cri-1: complete remission with incomplete hematological recovery one; CRi-2: complete remission with incomplete hematological recovery two; scSeq: single-cell sequencing.

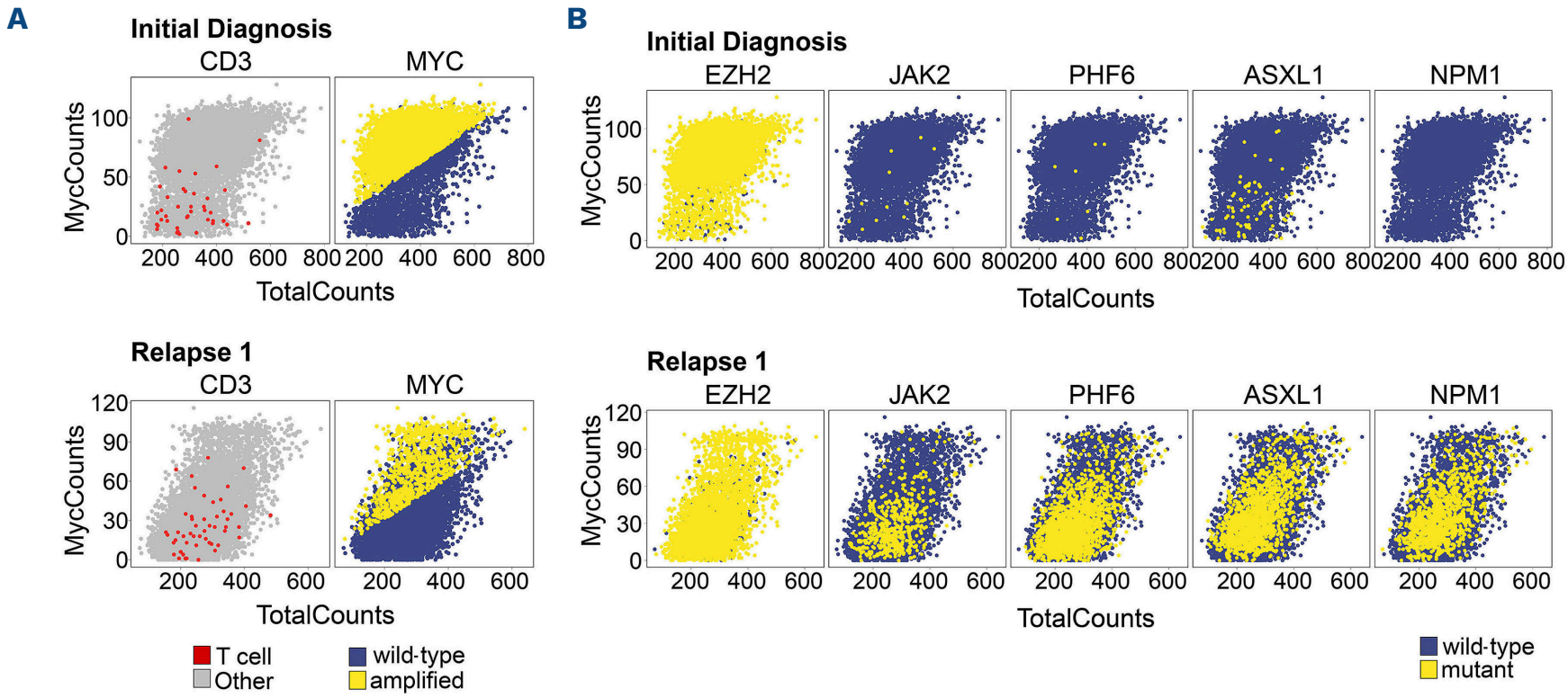

Continued on following page.

Figure 2. Single-cell DNA sequencing analysis. (A) Dot plots showing total counts on the x-axis and *MYC* counts on the y-axis, as well as highlighted in color the cell type (left panels: red: T cells, gray: other cells) or mutational status (right panels: blue: wild-type, yellow: *MYC*-amplified) at the indicated time points initial diagnosis (top) and relapse (bottom). (B) Dot plots showing total counts on the x-axis and *MYC* counts on the y-axis, as well as highlighted in color the mutational status (blue: wild-type, yellow: mutant) at the indicated time points initial diagnosis (top) and relapse (bottom). (C-E) Heatmaps showing the mutational status for the indicated genes at first diagnosis (C), remission 1 (D), and at relapse (E). Cells with dropout in any of the genes were removed, and the cells were additionally annotated with the expression of surface proteins (CD34, CD7, CD3, CD14) measured with cellular indexing of transcriptomes and epitopes by sequencing (CITE-seq). (F) Schematic of the clonal evolution as detected through single-cell DNA sequencing.

(Figure 2D) strongly suggested that *ASXL1* occurred downstream of the *EZH2* mutation.

In the second remission sample post consolidation two (CRi-2) *MYC*amp was detectable at a very low rate by scSeq, while FISH was still negative. The *JAK2* clone increased in abundance (25%), continued to co-occur with the *EZH2* p.T683A variant, but did not overlap with *MYC*amp cells (Table 1). In addition, a new *PHF6* mutation (p.Y103stop) was detected in 10% of cells. These cells shared the *EZH2* p.T683A, but they were devoid of the *JAK2* mutation and *MYC*amp. Of note, blasts were below 5% at this stage and flow cytometry did not detect the leukemia-associated immunophenotype from initial diagnosis, so that the patient was considered flow MRD-negative.

In the cytologic relapse sample, which was acquired 6 months later, *MYC*amp was detectable again by scSeq (12%; Figure 2E, F). The *JAK2* clone had decreased from 25% to 7%, while the *PHF6*-mutated cells represented the second largest clone at relapse downstream of the *EZH2* mutation (22%). An *NPM1* TCTG-insertion was found in 15% of cells. Interestingly, the *NPM1*-mutated cells harbored the *ASXL1* mutation, which was already present at diagnosis independently of the other three clones (Figure 2E, F).

Several observations are remarkable in this scSeq study: an *EZH2* missense mutation p.T683A was detectable already at initial diagnosis and was shared by the initial *MYC*amp clone, but also by two distinct *JAK2*- and *PHF6*-mutated clones emerging during cytologic remission. Based on the in-depth scSeq information this AML would have been classified as high-risk AML with myelodysplasia-related gene mutations (AML-MR) according to the new World Health Organization (WHO) and ELN 2022 classification, so that a therapy with CPX-351 would have been recommended.[1]

While the *JAK2*-mutated clone decreased from remission to relapse, the *PHF6*-mutated clone became the second largest subclone downstream of the *EZH2* mutation at relapse potentially pointing towards clonal selection during the maintenance therapy with glasdegib. *PHF6* mutations in AML are often frameshift or nonsense mutations.[9] As *PHF6* is an X-linked gene, these alterations are predominantly found in males as in our patient. *PHF6* mutations are associated with immature AML (FAB subtypes M0–M2).[9] Moreover, *PHF6* along with other epigenetic regulators such as *DNMT3A*, *TET2*, and *ASXL1*, is frequently altered in patients with clonal hematopoiesis.[9]

Genomic amplifications, such as dmin, homogeneously staining regions (hsr), are rare in leukemia, accounting for less than 1% of cytogenetically abnormal hematological malignancies and are associated with elderly patients and poor prognosis.[10] While we found *MYC*amp in form of dmin at initial diagnosis by FISH, the relapse sample revealed a novel trisomy 8 involving the *MYC* locus confirming the hypothesis that different *MYC*amp mechanisms can co-exist within the same leukemic cell population as previously described.[11] scSeq was able to detect *MYC*amp in both conditions, and the fraction of cells highly corresponded to the fractions detected by FISH or cytogenetics. *MYC* mutations have been reported to coincide with other mutations in AML, such as *FLT3*, *NPM1*, and *DNMT3A* mutations.[12] The interesting observation in this case is, that the additional clones developing during therapy did not occur in the *MYC*amp clone as expected. This might suggest, that the *MYC*amp clone facilitated development of the other AML clones by paracrine mechanisms, e.g., via BM niche remodeling.

Another striking observation in this case is the occurrence of a therapy-associated *NPM1* mutation. Approximately 15% of therapy-related AML cases carry *NPM1* mutations, frequently accompanied by a normal karyotype and *DNMT3A* mutations, and rarely associated with chromosome aberration.[13] Cases of *NPM1*-mutated AML following chemotherapy for previous lymphoid malignancies appear to arise from a background of *DNMT3A*- or *TET2*-driven clonal hematopoiesis (CH) rather than being a direct result of cytotoxic therapy.[14] It is therefore remarkable, that the *NPM1* mutation in this case occurred in cells harboring mutations in two other epigenetic regulators, ASXL1 and EZH2, suggesting a common mechanism. The *ASXL1*-mutated background and the co-existence of *NPM1* wild-type clones might explain the non-response to aza-ven in this case.

In summary we present a very unusual AML case with emergence of multiple parallel genetic clones during remission after treatment with intensive chemotherapy and targeted drugs including the hedgehog inhibitor glasdegib and the CD33-directed antibody “GO”. The complex clonal evolution observed in this case resulted in a very aggressive and multi-refractory disease, which raises the question, whether and how the agents applied might have contributed to clonal selection or exit from dormancy. These findings underscore the importance of employing scSeq to dissect individual cases, which can offer valuable mechanistic insights and help optimize therapeutic strategies.

Authors

Sonia Jaramillo,[1] Michael Scherer,[2] Chelsea Szu-Tu,[2] Sergi Beneyto-Calabuig,[2] Carsten Müller-Tidow,[1,3] Richard F. Schlenk,[1,4] Michael Hundemer,[1] Lars Velten[2,5] and Caroline Pabst[1,3]

[1]Department of Internal Medicine V, Heidelberg University Hospital, Germany; [2]Center for Genomic Regulation (CRG), The Barcelona Institute of Science and Technology, Barcelona, Spain; [3]Molecular Medicine Partnership Unit (MMPU), University of Heidelberg and European Molecular Biology Laboratory, Heidelberg, Germany; [4]NCT-Trial Center, National Center of Tumor Diseases, Heidelberg University Hospital and German Cancer Research Center, Germany and [5]Universitat Pompeu Fabra (UPF), Barcelona, Spain

Correspondence:
C. PABST - Caroline.Pabst@med.uni-heidelberg.de

https://doi.org/10.3324/haematol.2023.284922

Received: January 10, 2024.
Accepted: May 20, 2024.
Early view: May 30, 2024.

©2024 Ferrata Storti Foundation
Published under a CC BY-NC license

Disclosures

No conflicts of interest to disclose.

Contributions

CP and SJ designed the study, performed clinical data analysis and wrote the manuscript. MS, LV, CST, and SBC performed single cell sequencing and data analysis. MH performed the clinical diagnostics. SJ, RS, and CMT designed the clinical study. All authors contributed to writing the manuscript.

Funding

This research was funded by the José Carreras Leukaemia Foundation (DJCLS 01SP/(12)2022). CP is supported by a Max-Eder grant of German Cancer Aid (70114435). The authors gratefully acknowledge the data storage service SDS@hd supported by the Ministry of Science, Research and the Arts Baden-Württemberg (MWK) and the German Research Foundation (DFG) through grant INST 35/1314-1 FUGG and INST 35/1503-1 FUGG. MS was supported through the Walter Benjamin Fellowship funded by Deutsche Forschungsgemeinschaft (DFG, German Research Foundation) – 493935791.

Data-sharing statement

The authors welcome requests for the original data related to the laboratory analysis results.

References

1. Dohner H, Wei AH, Appelbaum FR, et al. Diagnosis and management of AML in adults: 2022 ELN recommendations from an international expert panel. Blood. 2022;140(12):1345-1377.
2. Jaramillo S, Krisam J, Le Cornet L, et al. Rationale and design of the 2 by 2 factorial design GnG-trial: a randomized phase-III study to compare two schedules of gemtuzumab ozogamicin as adjunct to intensive induction therapy and to compare double-blinded intensive postremission therapy with or without glasdegib in older patients with newly diagnosed AML. Trials. 2021;22(1):765.
3. DiNardo CD, Pratz K, Pullarkat V, et al. Venetoclax combined with decitabine or azacitidine in treatment-naive, elderly patients with acute myeloid leukemia. Blood. 2019;133(1):7-17.
4. Pellegrino M, Sciambi A, Treusch S, et al. High-throughput single-cell DNA sequencing of acute myeloid leukemia tumors with droplet microfluidics. Genome Res. 2018;28(9):1345-1352.
5. Beneyto-Calabuig S, Merbach AK, Kniffka JA, et al. Clonally resolved single-cell multi-omics identifies routes of cellular differentiation in acute myeloid leukemia. Cell Stem Cell. 2023;30(5):706-721.
6. Percy MJ, McMullin MF. The V617F JAK2 mutation and the myeloproliferative disorders. Hematol Oncol. 2005;23(3-4):91-93.
7. Bianchi A, Scherer M, Zaurin R, Quililan K, Velten L, Beekman R. scTAM-seq enables targeted high-confidence analysis of DNA methylation in single cells. Genome Biol. 2022;23(1):229.
8. Miles LA, Bowman RL, Merlinsky TR, et al. Single-cell mutation analysis of clonal evolution in myeloid malignancies. Nature. 2020;587(7834):477-482.
9. Van Vlierberghe P, Patel J, Abdel-Wahab O, et al. PHF6 mutations in adult acute myeloid leukemia. Leukemia. 2011;25(1):130-134.
10. Huh YO, Tang G, Talwalkar SS, et al. Double minute chromosomes in acute myeloid leukemia, myelodysplastic syndromes, and chronic myelomonocytic leukemia are associated with micronuclei, MYC or MLL amplification, and complex karyotype. Cancer Genet. 2016;209(7-8):313-320.
11. Abbate LA, Tolomeo D, Cifola I, et al. MYC-containing amplicons in acute myeloid leukemia: genomic structures, evolution, and transcriptional consequences. Leukemia. 2018;32(10):2152-2166.
12. Papaemmanuil E, Gerstung M, Bullinger L, et al. Genomic classification and prognosis in acute myeloid leukemia. N Engl J Med. 2016;374(23):2209-2221.
13. SanMiguel JM, Eudy E, Loberg MA, et al. Cell origin-dependent cooperativity of mutant Dnmt3a and Npm1 in clonal hematopoiesis and myeloid malignancy. Blood Adv. 2022;6(12):3666-3677.
14. Othman J, Meggendorfer M, Tiacci E, et al. Overlapping features of therapy-related and de novo NPM1-mutated AML. Blood. 2023;141(15):1846-1857.